geologica acta

Tectonic geomorphology of Bozdoğan and Karacasu grabens, western Anatolia

Erman Özsayin[1]   Kadir Dirik[1]   Faruk Ocakoğlu[2]   Sanem Açikalin Cartigny[3]   Azad Sağlam Selçuk[4]

[1]Hacettepe University, Department of Geological Engineering
06800, Ankara-Turkey. Özsayin E-mail: eozsayin@hacettepe.edu.tr   Dirik E-mail: kdirik@hacettepe.edu.tr

[2]Eskişehir Osmangazi University, Department of Geological Engineering
26040, Eskişehir-Turkey. Ocakoğlu E-mail: focak@ogu.edu.tr

[3]New Castle University, School of Natural and Environmental Sciences
Newcastle upon Tyne NE1 7RU–UK. Açikalin Cartigny E-mail: sanem.acikalin@ncl.ac.uk

[4]Van Yüzüncü Yıl University, Department of Geological Engineering
65080, Van-Turkey. Sağlam Selçuk E-mail: azadsaglam@yyu.edu.tr

┤ **A B S T R A C T** ├

Western Anatolia is one of the most rapidly extending and seismically active regions in the world. The circa N-S extension since the Early Miocene caused the formation of E-W trending major grabens and intervening horsts, having earthquake potentials with magnitude ≥5. The E-W oriented Büyük Menderes Graben cross-cuts the broadly N-S oriented Bozdoğan and Karacasu grabens, of which the boundary faults of the latter are the source of seismic activity. Geomorphic indices, including drainage basin asymmetry, mountain front sinuosity, valley-floor width to valley height ratio, stream length-gradient index and normalized channel steepness index, were used to evaluate the boundary fault segments of the Bozdoğan and Karacasu grabens. The results indicate that both grabens are tectonically active and therefore regions of earthquake potential, consistent with the epicenters of earthquakes. Thus, it can be inferred that fault segments of second-order grabens, which are crosscut by the boundary faults of seismically active main depressions, are apparently reactivated by ongoing tectonism and may represent seismic activity. This suggestion applies also for similar basins located in the western Anatolia.

KEYWORDS │ Karacasu Graben. Bozdoğan Graben. Geomorphic indices. Uplift rate. Seismic activity. Western Anatolia.

INTRODUCTION

Active tectonism has an important role in geomorphic processes, which in turn controls the density, pattern and geometry of the drainage system in the basin (Strahler, 1964) along with climate and lithology. Tectonically uplifted regions experience rejuvenation processes such as erosion, upward stream growing and existing channel incision (*e.g.* Jackson and Leeder, 1994; Keller and Pinter, 2002; Ouchi, 1985; Pérez-Peña *et al.*, 2010, 2015). The interplay between tectonics and drainage network geometry creates quantitatively measurable morphological features which help to determine the relative tectonic activity among the fault segments (Bull, 1977; Bull and McFadden,

1977; Keller, 1986; Keller and Pinter, 2002; Rockwell *et al.*, 1984). Morphological features such as mountain-front sinuosity, drainage basin shape and asymmetry of river channels are prominent and reliable tools to analyze the tectonic activity in continental extensional areas (Bull, 1977; Bull and McFadden, 1977; Keller, 1986; Keller and Pinter, 2002; Ramirez-Herrera, 1998; Silva *et al.*, 2003; Wells *et al.*, 1988).

The Western Anatolian Extensional Province (WAEP) is one of the world's most seismically active areas experiencing continental extension since the Early Miocene (McKenzie, 1978; Papazachos and Comninakis, 1971; Şengör and Yılmaz, 1981). The southern part of the WAEP is dominated by the E-W trending, few hundreds kilometer-scale Büyük Menderes Graben (BMG), along with less-pronounced, grossly N-S oriented cross-grabens such as Söke, Çine, Bozdoğan, Karacasu and Denizli (*e.g.* Kaymakcı, 2006; Ocakoğlu *et al.*, 2007; Sümer *et al.*, 2013) (Fig. 1A, B). This region has registered devastating historical earthquakes (Ergin *et al.*, 1967; Ocakoğlu *et al.*, 2013; Soysal *et al.*, 1981; Yönlü *et al.*, 2010).

The WAEP is a perfect natural laboratory for understanding the interaction between active tectonics and related morphological features such as linear mountain-fronts, deeply-incised valleys and migrated river channels. The Bozdoğan (BG) and Karacasu (KG) grabens are such depressions with active boundary faults (Duman *et al.*, 2011; Emre *et al.*, 2011) and associated morphological features. Although, several morphometry studies have been carried out in the region (*e.g.* Özkaymak, 2014; Özkaymak and Sözbilir, 2012; Özsayın, 2016; Topal, 2019a), only Topal (2019b) deals with the western margin of the Karacasu graben.

The aim of this study is to i) evaluate the fault segments of the BG and KG as a whole in terms of geomorphic indices, ii) assess the relative activity potential among the fault segments and iii) discuss the seismicity of the BG and KG in a regional perspective. For this aim, we mapped the boundary faults and juxtaposing rock units in the field and we performed morphotectonic and drainage analysis using GIS based software which comprise asymmetry factor, mountain-front sinuosity, valley-floor to valley-height ratio and channel normalized steepness index, for a better understanding the tectonic activity along the two cross-grabens.

GEOLOGICAL SETTING

Western Anatolia

The south/southwestwards movement of the Anatolian plate over the African plate along the Aegean-

Cyprian subduction zone led to the formation of the WAEP, characterized by a NNW-SSE tensional stress regime (McKenzie, 1978; Papazachos and Comninakis, 1971; Şengör and Yılmaz, 1981) (Fig. 1A). The approximately E–W trending Gediz, Küçük Menderes and Büyük Menderes grabens and the intervening horsts, are the main structures formed under this stress regime (Fig. 1B). Geodetic velocity measurements along with structural and seismic studies show that the WAEP is deformed by high strain rates by the active faults, generating dense seismicity in the region (*e.g.* Barka and Reilinger, 1997; Doğru *et al.*, 2014; Kahle *et al.*, 1998; Kurt *et al.*, 1999; Özener *et al.*, 2013). The earthquakes 1933 Çivril (Denizli) (M: 5.7), 1939 Dikili (İzmir) (M: 6.6), 1941 Muğla (M: 6.0), 1949 Karaburun (İzmir) (M: 6.6), 1955 Söke (Aydın) (M: 6.8), 1965 Denizli (M: 5.7) and 2020 Samos (M: 6.9) are the largest recorded events of the instrumental era (earthquake magnitudes are obtained from www.koeri.boun.edu.tr) while numerous devastating historical earthquakes have also been documented for the historical period (*e.g.* Altunel *et al.*, 2003; Ocakoğlu *et al.*, 2013).

Bozdoğan and Karacasu Grabens

The BG and KG are two depressions, located at the central part of the Büyük Menderes Graben and orthogonally cross-cut by it (Fig. 1C). The BG is approximately 40km long and 5–10km wide. The northern to central part of this graben has N–S-trending margins, whereas the central to southern parts display a southeasterly curvature. The average altitude of the central part of the graben is 85m while the highest peak reaches up to 1725m (Mt. Madran) at the SW of Bozdoğan village. The main drainage in the graben is the Akçay River.

The KG is approximately 35km long and 5–7km wide, and is located at the east of the BG; it is separated from it by the Karıncalıdağ horst. The graben has a NNW-SSE orientation at the junction point with the BMG where a smoother southeasterly curvature appears at the east of Karacasu village. The NNE-SSW trend gradually changes to an E-W trend at the southernmost part of the graben. The average altitude of the central part of the graben is 250m and the highest part is about 1500m (Mt. Karıncalıdağ). The Dandalas River constitutes the main drainage system of the KG.

The rock units exposed along the BG and KG are: basement units, Miocene clastic deposits and modern graben infill. Basement units are composed of Precambrian migmatite/gneiss, Paleozoic marble/quartz-schist and Mesozoic marble/schist (Bozkurt and Oberhansli, 2001; Konak and Göktaş, 2004). In both grabens, Miocene clastic deposits occur near the margins, unconformably overlying
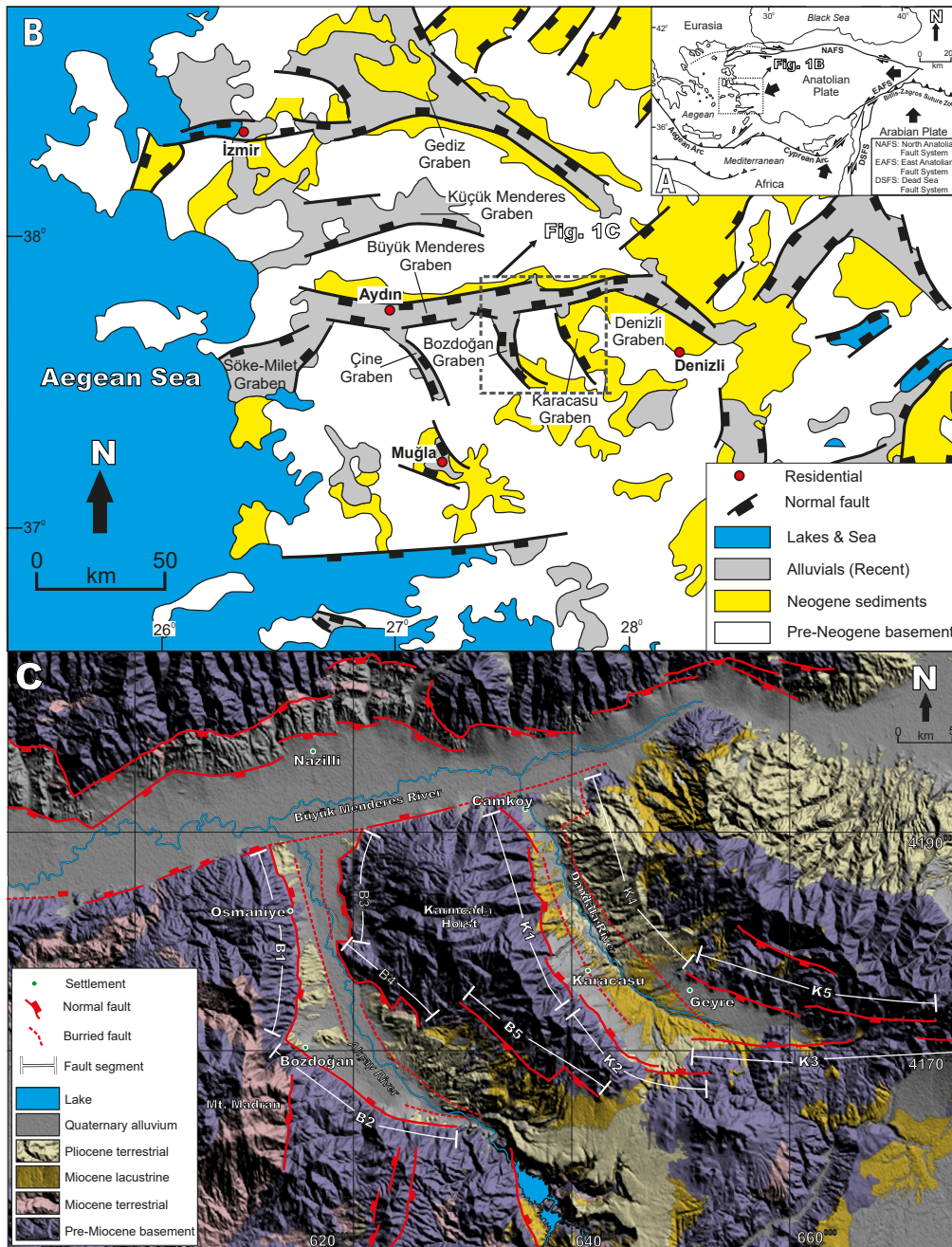
Figure 1. A) Simplified map of Turkey and surrounding area showing major neotectonic structures (simplified from Bozkurt, 2001). B) Simplified geological map of western Turkey showing the major grabens (adapted from Bozkurt and Mittwede, 2005). C) Geological map of the study area on a digital elevation model showing the segments of the boundary faults of Bozdoğan and Karacasu grabens (adapted from Ocakoğlu *et al.*, 2014).

the basement units. These clastic deposits interfinger with lacustrine mudstone-limestone alternations towards the center of the grabens (Açıkalın, 2005; Alçiçek, 2010; Alçiçek and Jiménez-Moreno, 2013; Becker-Platen, 1971; Kastelli, 1972; Nebert, 1955; Ocakoğlu *et al.*, 2014). Axial fluvial system deposits and alluvial fans of the modern graben infill cover the older units with a regional unconformity, which are deeply incised by the drainage system (Ocakoğlu *et al.*, 2015).

MATERIAL AND METHODS

In order to quantitatively evaluate the topographic response to active tectonics in the study area, we used several geomorphic indices, along with our field data. To calculate the geomorphic indices for the BG and KG, 1:25.000 scale topographic maps and the 30-m ASTER GDEM (Global Digital Elevation Model) data (available at http://www.gdem.aster.ersdac.or.jp) were used. ArcGIS (ver. 10.8)

Table 1. Summary of the morphometric parameters used in this study (modified from Özkaymak, 2014)

Morphometric parameter	Mathematical derivation [a]	Measurement procedure	Explanation	Source
Smf, Mountain front sinuosity	$Smf = Lmf/Ls$	(Plan view)	Reflect a balance between the tendency of stream and slope processes to produce irregular (sinuous) mountain front and vertical active tectonics that tend to produce a prominent straight front. *Smf*>1.4–most tectonic activity; *Smf*>1.4–less tectonic activity	(1, 2, 3, 4, 5, 6)
Vf, valley floor width-to height ratio	$Vf= 2Vfw/[(E\ ld- Esc) + (Erd- Esc)]$	(cross section)	Define the ratio of the width of the valley floor to the mean height of two adjacent divides. The index reflects differences between broadfloored canyons with relatively high values of *Vf*, and V-shaped canyons with relatively low *Vf* values	(2, 3, 4)
SL, Stream length-gradient index	$SL = (\Delta H/\Delta L)\cdot L$	(block diagram)	Total or available stream power is related to the slope of the water channel. Sudden changes in *SL* values along the stream channel indicate lithological differences and/or possible tectonic activity	(3, 5, 7, 8)
Ksn, Normalized channel steepness index	$S = Ks\cdot A^{-\theta}$		Define the channel slope if it is unexpectedly steep or gentle with respect to its drainage area. Normally, the channel slope decreases with drainage area. Existing of knickpoints show sudden increases along slope profiles that may be related to lithological changes and/or tectonic uplift.	(9, 10)
T, Transverse topographic symmetry factor	$T = Da/Dd$	(Plan view)	Shows the tectonic tilting of the drainage basin. For symmetrical basins, *T*=0. If asymmetry increases *T* values increase and reach to 1. Migration direction of stream from basin midline indicates the active segment(s) of the basin bounding faults.	(3)
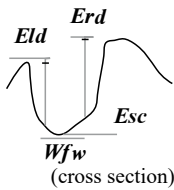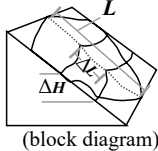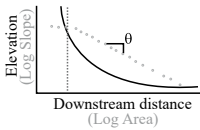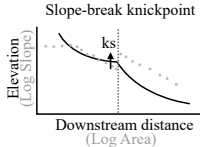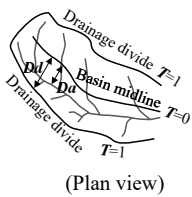
Sources: (1) Bull (1977); (2) Bull and McFadden (1977); (3) Keller and Pinter (2002); (4) Silva *et al.* (2003); (5) El Hamdouni *et al.* (2008); (6) Rockwell *et al.* (1984); (7) Hack (1973); (8) Alipoor *et al.* (2011); (9) Kirby and Whipple (2012); (10) Boulton *et al.* (2014). Symbols: **Lm:** length of mountain front along the mountain-piedmont junction; **s**: straight-line length of the front; **Vfw:** width of valley floor; **Eld** and **Erd:** respective elevations of the left and right valley divides; **Esc:** elevation of the valley floor; **ΔL**: length of the reach; **ΔH**: height of reach; **L**: total channel length from the point of interest where the index is being calculated upstream to the highest point on the channel; **Da**: distance from the basin midline to the midline of the meander belt; **Dd**: distance from the basin midline to the basin divide.

and TecDEM toolbox with Matlab™ (ver. 2014b) software were used for computing the stream network and related calculations. Selby's (1980) rock strength classification and a 1:25.000 scale geological map of the study area (Ocakoğlu *et al.*, 2014) were used to estimate the effect of lithological variations. According to this classification, metamorphic basement (Precambrian migmatite/gneiss, Paleozoic marble/quartz-schist and Mesozoic marble/ schist) have very high strength, whereas Miocene continental clastic rocks and lacustrine deposits have high and moderate strength, respectively. Pliocene terrestrial clastic rocks have low strength, and recent alluvial deposits

have likely very low strength. The fault segments of both grabens are numbered and investigated separately based on their orientations and step over zones (Fig. 1C).

The geomorphic indices used in this study include the transverse topographic symmetry factor (*T*), mountain-front sinuosity (*Smf*), valley-floor width to valley height ratio (*Vf*), stream-length gradient index (*SL*) and normalized channel steepness index (*Ksn*). *T* determines the migration of the river channel due to tectonic activity along the drainage basin. For perfectly symmetrical basins *T=0*, which represents negligible influence of fault activity. In asymmetrical basins *T* values reach up to 1, which means the main river channel migrated towards the active fault segment bounding the basin (Keller and Pinter, 2002) (Table 1).

Mountain-front sinuosity (*Smf*) is a useful tool for evaluating and comparing active fault segments, reflecting the balance between tectonic activity and erosional forces. High tectonic activity and related uplift prevail over erosional processes, creating straight mountain-fronts (low *Smf* values). When tectonic activity is reduced erosional processes make mountain-fronts more sinuous (high *Smf* values) (Keller and Pinter, 2002) (Table 1). *Vf* is a geomorphic tool for estimating valley incision between fault segments. Higher tectonic activity and uplift rates will bring out deeply incised, V-shaped valleys with lower *Vf* values. But in erosion-dominated areas, the valleys are broad-floored and U-shaped with higher *Vf* values (Bull and McFadden, 1977; Keller and Pinter, 2002) (Table 1). *SL* describes the stream channel slope along the river bed, identifying sudden slope changes due to erosional differences among lithological boundaries and/or fault activity. Low *SL* values indicate gentle slope along the channel whereas high values correspond to sudden drops (Keller and Pinter, 2002) (Table 1). *Ksn* determines slope gradient anomalies along the river profiles (Ouimet *et al.*, 2009; Whittaker, 2012). Normally, in a typical drainage basin, the slope of the river channel gradually decreases downward. This can be modified by lithological boundaries where rock resistance to erosion differs or by active faulting, creating a vertical displacement. The exponential relationship between channel slope (*S*) and upstream area (*A*) in graded rivers are defined as power-law (Hack, 1957), which is expressed by:

$$S = Ks A^{-\theta}$$

where *Ks* is the channel steepness-index and θ the concavity index (Flint, 1974). Variations such as active tectonics, climate and river bed lithology directly affects the slope of the channel and upstream area, changing the *Ks* and θ in the equation (Kirby and Whipple, 2012;

Wobus *et al.*, 2006). For the determination of *Ks* and θ in a river profile is to execute regressions in logarithmic slope-area plots (Ferrater *et al.*, 2015) where these plots can be used to locate the knickpoints and distinct areas with different uplift (Burbank and Anderson, 2013; Kirby and Whipple, 2012; Whipple *et al.*, 2013; Wobus *et al.*, 2006). These knickpoints arise when constant changes take place in boundary conditions like base-level fall due to uplift rate changes or diversification in climatic conditions (Bishop *et al.*, 2005; Kirby and Whipple, 2012; Snyder *et al.*, 2003). Previous studies indicate that the concavity index (θ) range between 0.4 and 0.6 in most cases and is relatively unaffected by tectonism, lithological changes and/or climate (Kirby and Whipple, 2012; Whipple *et al.*, 2013). "Normalized" steepness index (*Ksn*) method is used for river reaches with fixed "reference" concavity (Wobus *et al.*, 2006) which has been used in morphometric studies (*e.g.* Camafort *et al.*, 2020; Ferrater *et al.*, 2015; Kirby and Whipple, 2012; Sağlam-Selçuk and Kul, 2021; Whipple *et al.*, 2013; Wobus *et al.*, 2006). Thus, the θ value is taken as 0.5 during the calculations on TecDEM toolbox analysis (Table 1).

RESULTS

Transverse topographic symmetry factor (*T*)

T values in the BG range from 0.07 to 0.69. Low *T* values are found along the B1 segment (NW of the graben) whereas high values are found in the B2 segment (SW of the graben). These results suggest that the BG is tilted to the southwest (Fig. 2). In the KG, *T* values vary between 0.14 and 0.53. K1 and K4 segments (NW and NE of the graben respectively) display relatively high *T* values, indicating northeastern tilting. K2 and K3 segments (SE and S of the graben respectively) have low *T* values, indicating southwestern tilting (Fig. 2).

Mountain-front sinuosity (*Smf*)

Smf values in the BG vary between 1.41 and 2.07 (Fig. 3; Table 2). The lower values are found in the B1 and B2 segments. In the KG, *Smf* values range from 1.43 to 2.59 (Fig. 3; Table 2). Western and southern segments (K1, K2 and K3) present the lower values.

Ratio of valley-floor width to valley height index (*Vf*)

Mean and median *Vf* values were calculated for all valleys in the BG and KG. In the BG, *Vf* (mean) values vary between 0.30 and 0.60 (Fig. 3; Table 2). Low values are found in the B1 and B2 segments, indicating V-shaped valleys, whereas in the B3, B4 and B5 segments values are
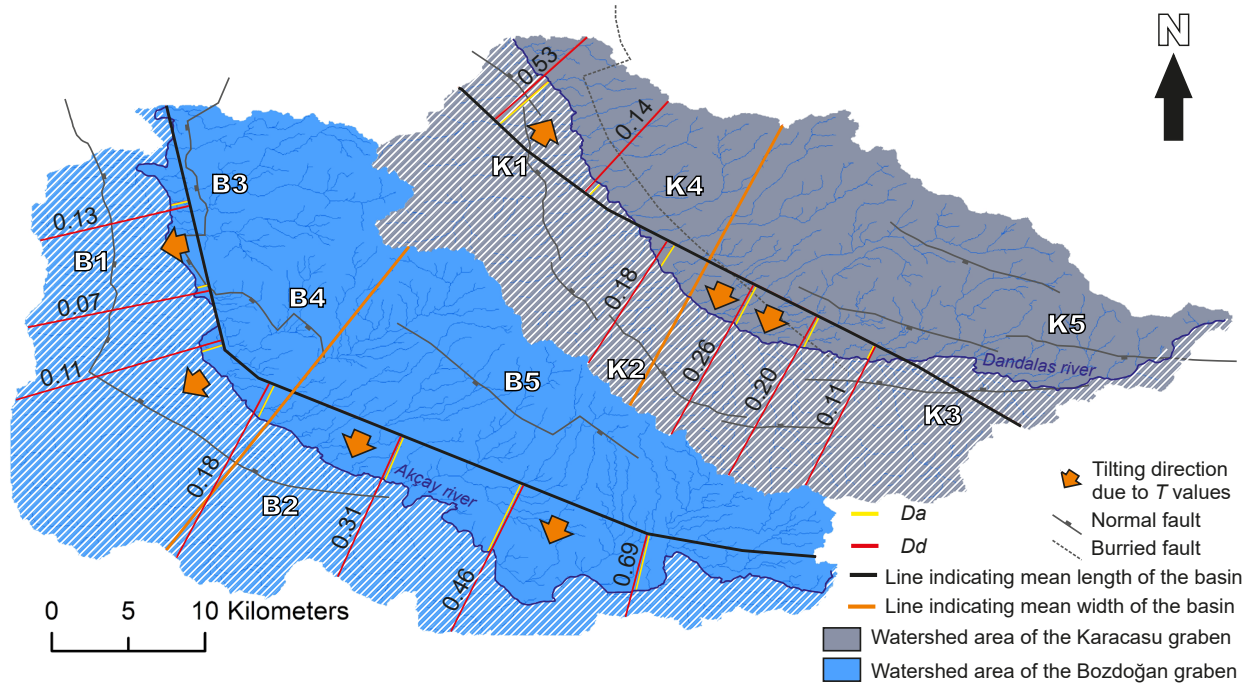
Figure 2. Schematic map of the study area showing the values of the transverse topographic symmetry factor (*T*). Striped areas are the western-southwestern part of Bozdoğan and Karacasu grabens. Numbers on red lines indicate *T* values along the line.

high, indicating U-shaped valleys. In the KG, *Vf* (mean) values vary between 0.18 and 0.75 (Fig. 3; Table 2), the lower values are found in the K1 segment, suggesting V-shaped valleys, whereas in the K2, K3 and K5 segments (V- and U-shaped valleys) have similar values.

Stream length-gradient index (*SL*)

SL values of streams cutting the fault segments range between 0.9 and 1875. Low *SL* values are found in the main drainage of the BG and upstream ends of the drainage
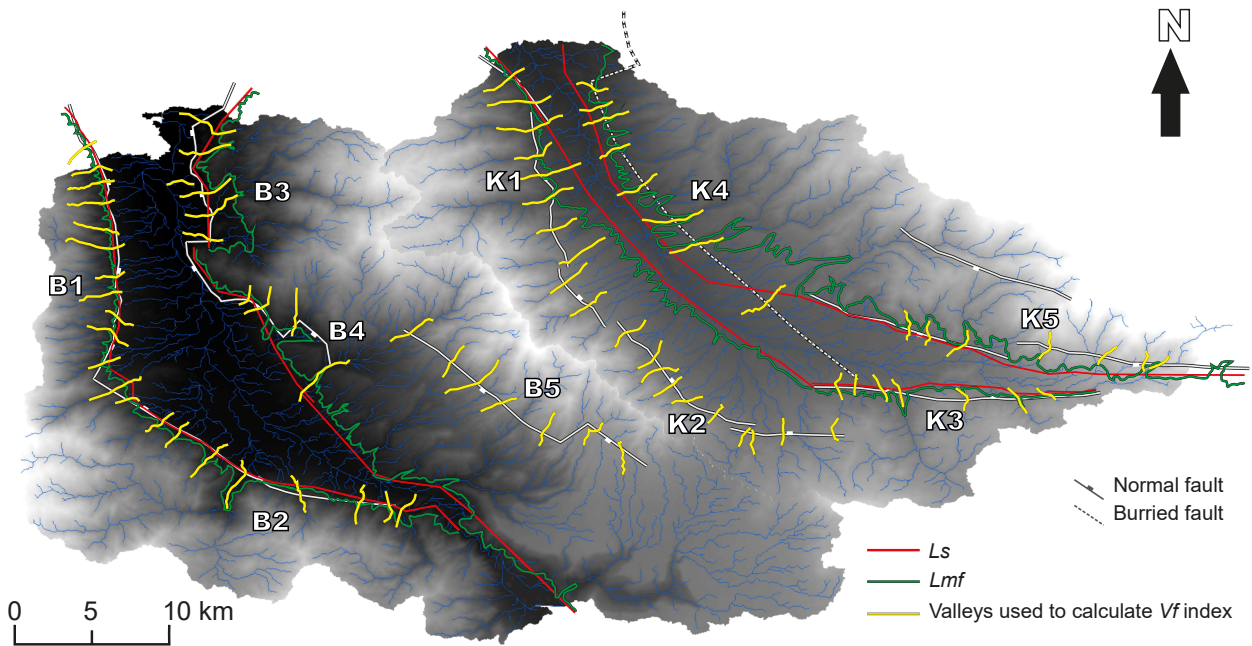

Figure 3. Schematic watershed map of the study area showing the *Smf* and *Vf* lines used for the calculation.

| 6 |

Table 2. Morphological properties of the main segments and basins of the Bozdoğan and Karacasu grabens, showing *Smf* (mountain front sinuosity ratio) and *Vf* (valley floor width-to-height ratio)

Segment no	*Smf*	*Vf* (mean)	Standart Deviation (*Vf*)
B1	1.41	0.30	0.11
B2	1.57	0.33	0.13
B3	2.07	0.56	0.30
B4	1.67	0.57	0.27
B5	1.80	0.60	0.22
K1	1.62	0.18	0.08
K2	1.56	0.40	0.22
K3	1.43	0.45	0.27
K4	2.59	0.75	0.58
K5	1.92	0.43	0.13

basins. In the BG, *SL* values gradually increase along the B1 and B2 segments (Fig. 4), probably indicating a change in rock strength where basement units and basinfill deposits juxtapose. Maximum *SL* values are found at the northwestern part of the B2 segment. *SL* values along the B3 segment are also high, particularly at the central part of the segment. B4 and B5 segments show relatively low values, which is typical of lithological changes (Fig. 4). *SL* values in the KG are higher than those obtained in the BG. Highest values are found at the northern part of the graben,

mostly in the K1 segment. Here, high *SL* values reflect both lithological changes and normal faulting (Fig. 4). Central to southeastern part of the K4 segment (where K4 and K5 segments overlap) also exhibits relatively high *SL* values. *SL* values in the K2, K3 and K5 segments are relatively low and variation in values are mostly related to the change in rock strength. Only easternmost parts of K3 and K5 locally show faulting-related changes.

Normalized Channel Steepness Index (*Ksn*)

Highest *Ksn* values (*Ksn* >400) are found in the southwestern part of the BG (western and southwestern part of B2) and western part of the KG (western part of K1). *Ksn* values are high on the western blocks of both grabens and medium values are found in their footwalls (Fig. 5A). Additionally, *Ksn* values increase (>400) at the southern part of the study area. Medium *Ksn* values are mostly obtained from the footwalls of the fault segments in both grabens while lower values are located at the hanging walls (Fig. 5A).

DISCUSSION

Interpretation of geomorphic indices and relative tectonic activity assessment of segments

In this study, five morphometric indices, including transverse topographic symmetry factor (*T*), mountain-front sinuosity (*Smf*), ratio of valley-floor width to valley height
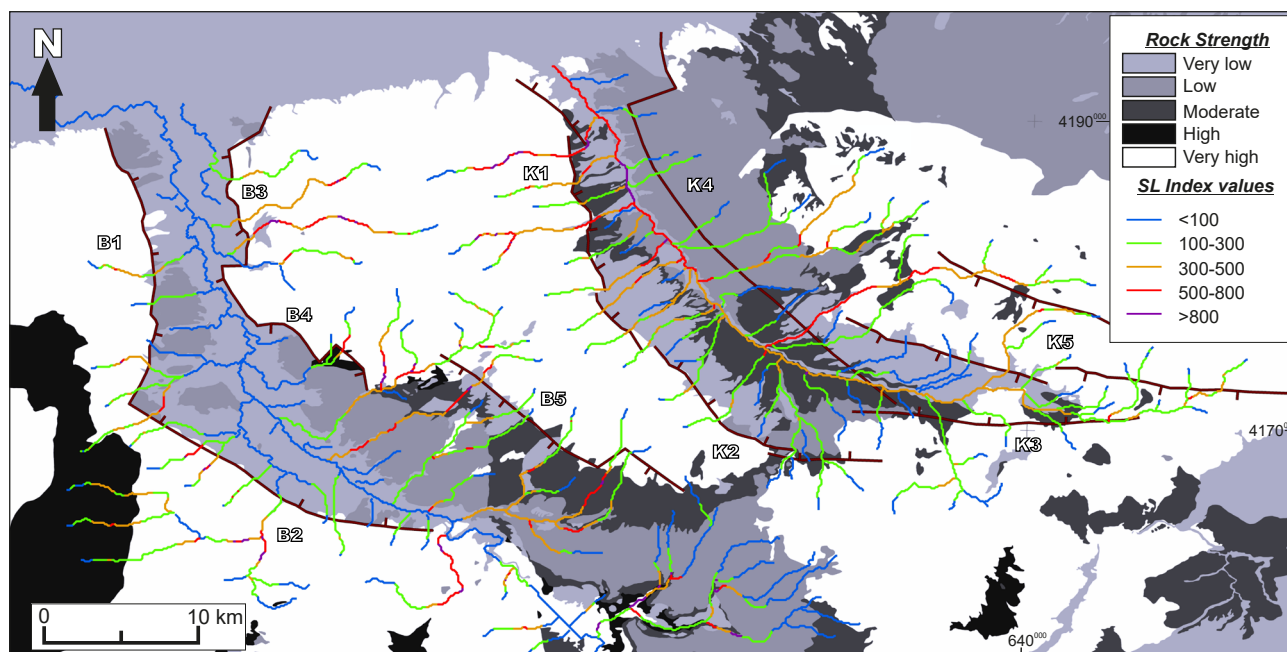

Figure 4. Simplified map of the study area showing the *SL* index values along the drainage of Bozdoğan and Karacasu grabens. Selby's (1980) rock strength classification was used to classify the rock units.
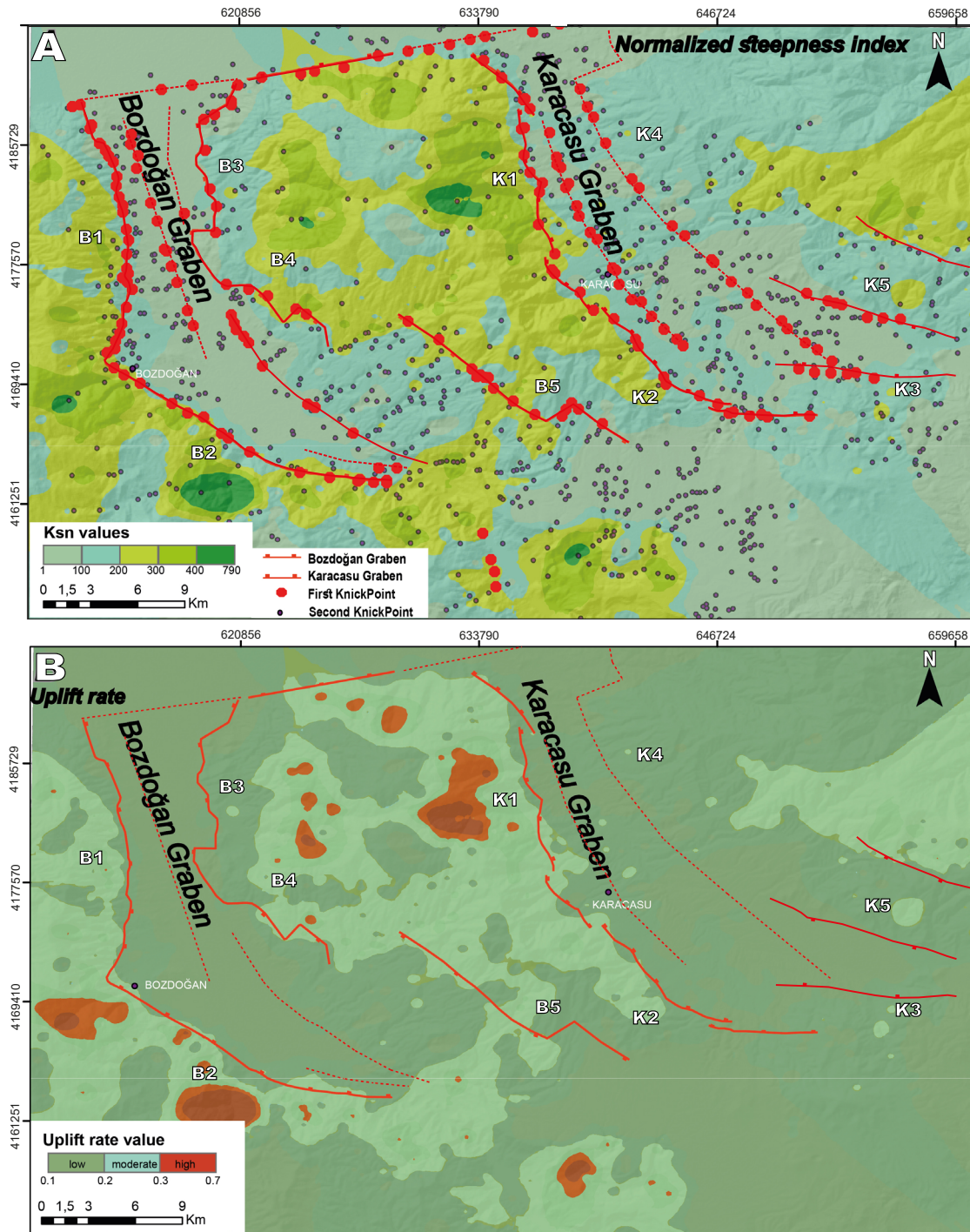
Figure 5. A) Sensitivity map of the normalized channel steepness index (Ksn) of the study area to tectonic activity. B) Simplified map of the study area showing the calculated uplift rates.

(*Vf*), stream-length gradient index (*SL*) and normalized channel steepness index (*Ksn*) are applied to the boundary faults of the BG and KG.

T values in the BG represent westward/southwestward tilting which suggests relatively higher activity on B1 and B2. Similarly, in the KG, *T* values suggest southwestern tilting along K1, K2 and K3 segments. This fact may be related to reactivation of the boundary faults of both grabens. In previous studies, these grabens were called "cross-grabens" which initiated as half-grabens with active western margins and later evolved to grabens with
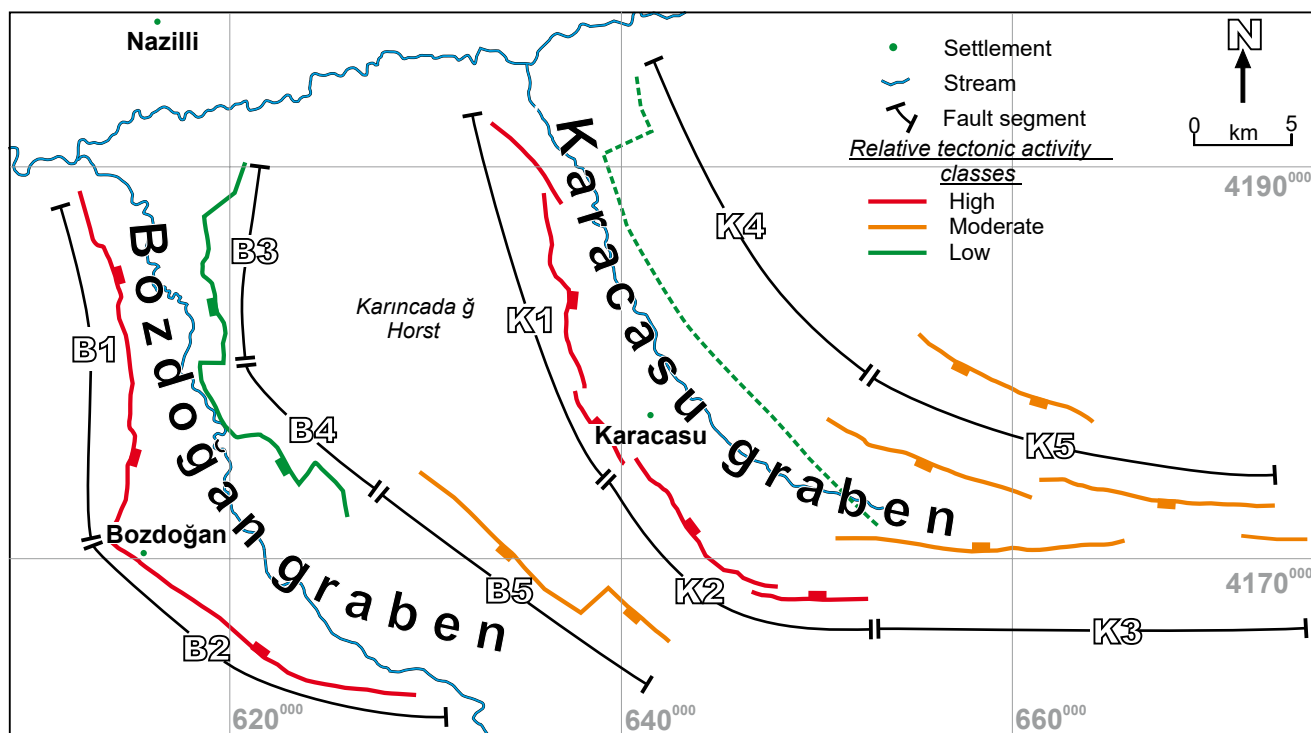
Figure 6. Simplified map of the study area showing the main segmentation of the grabens. Color codes of the faults indicate relative tectonic activity classes.

relatively less active eastern margins (Alçiçek, 2010; Yılmaz *et al.*, 2000).

Low *Smf* values, that represent high tectonic activity, were found in the western and southwestern segments of both grabens. These segments present relatively straight mountain fronts. High *Smf* values, that indicate low tectonic activity, were mostly found in the eastern and southern segments of the BG and KG. *Vf* values were similar in both grabens, demonstrate similar results with *Smf*, referring that B1 and B2 segments of the BG and, K1, K2 and K3 segments of the KG have relatively higher activity.

SL values support the results of other geomorphic indices. High *SL* values obtained in the B1 and B2 segments suggest high activity in the western/southwestern margin of the BG. In the KG, dominating segment is K1 and displays highest *SL* values. Additionally, the overlapping part between K4 and K5 has the same properties. Although, the two grabens have the same lithology and display similar boundary morphologies, *SL* indices were higher in the KG. These results are compatible with those of Topal (2019a) and Ocakoğlu *et al.* (2007) indicating western/southwestern margins of the basins representing relatively higher activity based on field studies and morphological interpretations.

Ksn results indicate three major areas with high *Ksn* values. Two of these areas are located in the western footwalls of both grabens and the third one in the southern part. As high *Ksn* values indicate high tectonic activity it can be inferred that the western margins have relatively higher tectonic activity, consistent with remaining morphometric analyses. The high values found in the southern part are thought to have generated from the rotational deformation of the area which created southeastern curvature of the BG and KG.

A relative uplift rate map was generated from the knickpoints, concavity and *Ksn* values (Fig. 5B). Relatively high uplift rate values were located at the footwall of the B2, B3, B4 and K1 segments (Fig. 5B). Uplift rates of these areas are greater than 0.4mm/yr. The high erosion rates observed in the western blocks of both grabens may show that the deformation changes along the fault segments are related with the strike of the segments forming the southeastern curvature. These uplift rates are compatible with the middle-late Pliocene uplift rates (0.2-0.3mm/yr) suggested for the Western Anatolian Extensional Province (Demir *et al.*, 2004), the Pliocene-Quaternary uplift rates in the Büyük Menderes region (0.1-0.2mm/yr, Westaway *et al.*, 2003), and the uplift rates in the southern part of Denizli Graben (0.15-0.38mm/yr, Özkaymak, 2014), Çameli Basin (0.05-0.5mm/yr, Özsayın, 2016), Kemalpaşa Basin (0.1–0.5mm/

yr, Tepe and Sözbilir, 2017), Priene-Sazlı Fault of Söke Basin (0.05-0.5mm/yr, Topal, 2019a) and in the Çamköy and Yazır segments of the KG (0.05-0.5mm/yr, Topal, 2019a).

In summary, the results of the calculated geomorphic indices mentioned above indicate that high tectonic activity should be expected in the B1 and B2 segments of the BG and in the K1 and K2 segments of the KG (Fig. 6). Moderate activity should be expected in the B5 segment of the BG and in the K3 and K5 segments of the KG. Low activity should be expected in the B3 and B4 segments of the BG and in the K4 segment of the KG. The highest relative activities are obtained from B1 segment of the BG and K1 segment of the KG, which are the closest segments and are both crosscut by the seismically active southern margin of the Büyük Menderes Graben.

Regional significance of the results and implications on seismic hazard

The Western Anatolia Extensional Province is one of the most seismically active regions in the world. The Kandilli Observatory and Earthquake Research Institute (KOERI) recorded 10.921 earthquakes with magnitude ≥3.0 in the Gediz, Küçük Menderes and Büyük Menderes grabens from the year 1901 to 2022 (Fig. 7). In addition, several historical earthquakes have also been recorded and documented in the BMG region (*e.g.* Altunel *et al.*, 2003; Ocakoğlu *et al.*, 2013; Soysal *et al.*, 1981; Yönlü *et al.*, 2010). Typically, the seismic activity is located along the Gediz and Büyük Menderes grabens, particularly at the eastern and western ends. Previous studies showed that the western margins of these grabens are terminated at the İzmir-Balıkesir Transfer Zone (Uzel *et al.*, 2013; Uzel and Sözbilir, 2008) where eastern margins are cut by the Uşak-Muğla Transfer Zone (Gessner *et al.*, 2017; Karaoğlu, 2014; Karaoğlu and Helvacı, 2014). As these zones are known to be the interconnecting structures, higher and complex activity is expected along these zones (Faulds and Varga, 1998).

Beside these junction points, the epicenters of the earthquakes are also concentrated along the margins of the main E-W trending grabens, predominantly at the
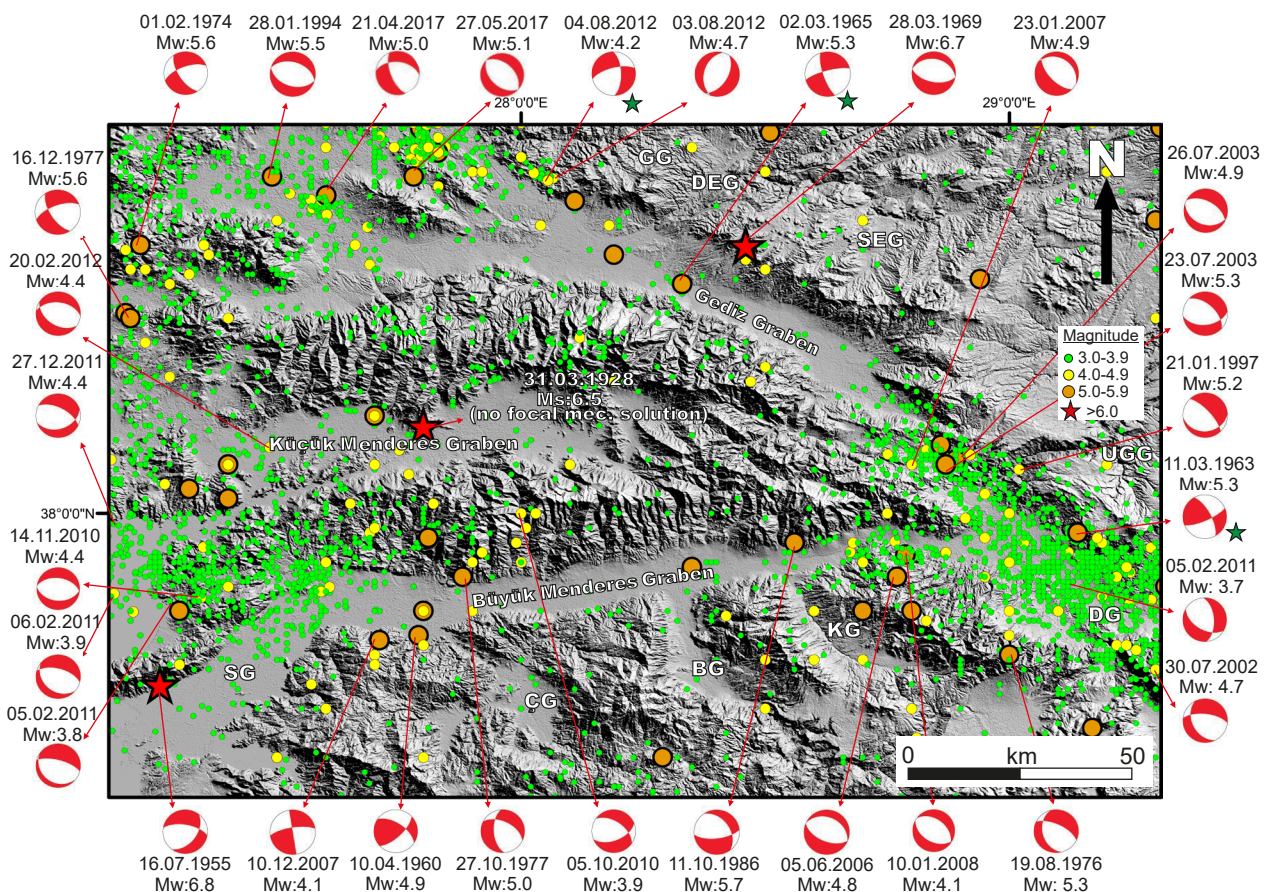

Figure 7. Digital elevation model of the Menderes massif showing the epicenters of earthquakes with magnitudes ≥3.0 (from 1901 to 2022) (SG: Söke graben, ÇG: Çine Graben, BG: Bozdoğan graben, KG: Karacasu graben, DG: Denizli graben, UGG: Uşak-Güre graben, SEG: Selendi graben, DEG: Demirci graben, GG: Gördes graben) (earthquake data is from www.koeri.boun.edu.tr).

intersection areas with the cross-cutting smaller grabens, such as the BG and KG. The epicenter distribution at the intersection of the KG and BG with the BMG and also along these smaller depressions are good examples of the relative activity due to the movements on the BMG. Similar activity can be observed in the Söke, Çine, Denizli, Uşak-Güre, Selendi and Gördes grabens that are terminated by the Büyük Menderes and Gediz grabens (Fig. 7). Some of the focal mechanism solutions differ from the dominant view (especially along the Gediz graben). This might be a consequence of reactivation of fault planes which were formed before neotectonic period.

Earthquakes magnitudes, located in BG and KG, range between 3.0 and 5.9. Topal (2019a) indicates that the Çamköy and Yazır segments of the KG have potential to produce earthquakes of magnitude M ≥6. But, taken into account the length of segments in the BG and KG, only the B1 and B2 segments of the BG have earthquake capacities with maximum magnitude M. 6.3 while remaining segments have M <6.0 according to Wells and Coppersmith (1994).

CONCLUSION

In this study, five geomorphic indices were analyzed in the Bozdoğan and Karacasu grabens, which are cross-cut by the active BMG. The morphometric analysis clearly indicated that, in both grabens, tectonic activity was higher in the western/southwestern margins than in the eastern boundary fault segments. Moderate activity was detected in the southeastern segments. The activity along the southeastern segments is probably related to the regional extension, as their orientation is very similar to that of the boundary fault segments of the BMG. The lowest activity was found in the almost N-S trending eastern segments of the grabens. In the eastern margin of the BG, valleys are U-shaped and mountain-fronts sinuous, which indicate low tectonic activity. The eastern margin of the KG, is defined by a buried fault dominated by v- to u-shaped valleys and low relief, pointing to intense erosion and low tectonic activity. As neighboring cross-grabens (*e.g.* Çine, Söke and Denizli grabens in the BMG; Gördes, Demirci, Selendi and Uşak-Güre grabens in the Gediz Graben) have quite similar geodynamic history to that experienced byf the BG and KG, it can be inferred that relatively higher activity should be expected from the similar segments of these depressions.

ACKNOWLEDGMENTS

REFERENCES

Açıkalın, S., 2005. Sedimentary evolution of the Karacasu cross-graben (Aydın, West Anatolia) (in Turkish with English abstract). MSc Thesis. Eskişehir (Turkey), Osmangazi University, 138pp.

Alçiçek, H., 2010. Stratigraphic correlation of the Neogene basins in southwestern Anatolia: regional palaeogeographical, palaeoclimatic and tectonic implications. Palaeogeography, Palaeoclimatology, Palaeoecology, 291, 297-318.

Alçiçek, H., Jiménez-Moreno, G., 2013. Late Miocene to Plio-Pleistocene fluvio-lacustrine system in the Karacasu Basin (SW Anatolia, Turkey): depositional, paleogeographic and paleoclimatic implications. Sedimentary Geology, 291, 62-83.

Alipoor, R., Poorkermani, M., Zare, M., El Hamdouni, R., 2011. Active tectonic assessment around Rudbar Lorestan damsite, High Zagros Belt (SW of Iran). Geomorphology, 128(1-2), 1-14.

Altunel, E., Stewart, I.S., Piccardi, L., Barka, A., 2003. Earthquake faulting at ancient Cnidus, SW Turkey. Turkish Journal of Earth Sciences, 12, 137-152.

Barka, A.A., Reilinger, R., 1997. Active tectonics of the Mediterranean region: deduced from GPS, neotectonic and seismic data. Annali di Geofisica, XI, 587-610.

Becker-Platen, J.D., 1971. Stratigraphic division of the Neogene and oldest Pleistocene in Southwest Anatolia. Newsletter on Stratigraphy, 1-3, 19-22.

Bishop, P, Hoey, T.B., Jansen, J.D., Artza, I.L., 2005. Knickpoint recession rate and catchment area: the case of uplifted rivers in Eastern Scotland. Earth Surface Processes and Landforms, 30(6), 767-778.

Boulton, S.J., Strokes, M., Mather, A.E., 2014. Transient fluvial incision as an indicator of active faulting and Plio-Quaternary uplift of the Moroccan High Atlas. Tectonophysics, 633, 16-33.

Bozkurt, E., 2001. Neotectonics of Turkey – a synthesis. Geodinamica Acta, 14, 3-30.

Bozkurt, E., Oberhansli, R., 2001. Menderes Massif (Western Turkey): structural, metamorphic and magmatic evolution - a synthesis. International Journal of Earth Sciences, 89, 679-708.

Bozkurt, E., Mittwede, S.K., 2005. Introduction: Evolution of Neogene extensional tectonics of western Turkey. Geodinamica Acta, 18(3-4), 153-165.

Bull, W.B., 1977. Tectonic geomorphology of the Mojave Desert, California. U.S. Geological Survey Contract Report 14-0-001-G-394. Office of Earthquakes, Volcanoes, and Engineering, Menlo Park, CA., 188pp.

Bull, W.B., McFadden, L.D., 1977. Tectonic geomorphology north and south of the Garlock fault, California. In: Doehering, D.O. (ed.). Geomorphology in arid regions. Proceedings of the Eighth Annual Geomorphology Symposium. Binghamton, State University of New York, 115-138.

Burbank, D.W., Anderson, R.S., 2013. Tectonic Geomorphology. Oxford, Blackwell Science, 2nd edition, 287pp.

Camafort, M., Pérez-Peña, J.V., Booth-Rea, G., Melki, F., Grácia, E., Azañón, J.M., Galve, J.P., Marzougui, W., Gaidi, S., Ranero, C., 2020. Active tectonics and drainage evolution in the Tunisian Atlas driven by interaction between crustal shortening and mantle dynamics. Geomorphology, 351, 106954.

Demir, T., Yeşilnacar, İ., Westaway, R., 2004. River terrace sequences in Turkey: sources of evidence for lateral variations in regional uplift. Proceedings of the Geologists' Association, 115, 289-311.

Doğru, A., Görgün, E., Özener, H., Aktuğ, B., 2014. Geodetic and seismological investigation of crustal deformation near İzmir (Western Anatolia). Journal of Asian Earth Sciences, 82, 21-31.

Duman, T.Y., Emre, Ö., Özalp, S., Elmacı, H., 2011. 1:25.000 scale Active Fault Map Series of Turkey, Aydın (NJ 35-11) Quadrangle Serial Number: 7, General Directorate of Mineral Research and Exploration, Ankara-Turkey.

Emre, Ö., Duman, T.Y., Özalp, S., Elmacı, H., 2011. 1:25.000 scale Active Fault Map Series of Turkey, Denizli (NJ 35-12) Quadrangle Serial Number: 12, General Directorate of Mineral Research and Exploration, Ankara-Turkey.

Ergin, K., Güçlü, U., Uz, Z., 1967. A catalogue of earthquakes for Turkey and surrounding area (11 A.D.–1964) [in Turkish]. Technical University of İstanbul, Publications, No. 24.

Faulds, J.E., Varga, R.J., 1998. The role of accommodation zones and transfer zones in the regional segmentation of extended terranes. Geological Society of America, Special Papers, 323, 1-45.

Ferrater, M., Booth-Rea, G., Pérez-Peña, J.V., Azañón, J.M., Giaconia, F., Masana, E., 2015. From extension to transpression: quaternary reorganization of an extensional related drainage network by the Alhama de Murcia strike-slip fault (eastern Betics). Tectonophysics, 663, 33-47.

Flint, J.J., 1974. Stream gradient as a function of order, magnitude, and discharge. Water Resources Research, 10, 969-973.

Gessner, K., Markwitz, V., Güngör, T., 2017. Crustal fluid flow in hot continental extension: tectonic framework of geothermal areas and mineral deposits in western Anatolia. In: Gessner, K., Blenkinsop, T.G., Sorjonen-Ward, P. (eds.). Characterization of Ore-Forming Systems from Geological, Geochemical and Geophysical Studies. London, The Geological Society, 453 (Special Publications), 289-311. DOI: 10.1144/SP453.7

Hack, J.T., 1957. Studies of longitudinal profiles in Virginia and Maryland. U.S. Geological Survey, United States Government Printing Office, Washington, Professional Paper 294-B, 1.

Hack, J.T., 1973. Stream-profile analysis and stream-gradient index. Journal of Research of the U.S. Geological Survey, 1(4), 421-429.

el Hamdouni, R., Irigaray, C., Fernández, T., Chacón, J., Keller, E.A., 2008. Assessment of relative active tectonics, southwest border of the Sierra Nevada (southern Spain). Geomorphology, 96, 150-173.

Jackson, J., Leeder, M., 1994. Pergamon drainage systems and the development of normal faults: an example from Pleasant Valley, Nevada. Journal of Structural Geology, 16, 1041-1059.

Kahle, H.G., Straub, C., Reilinger, R., McClusky, S., King, R., Hurst, K., Veis, G., Kastens, K., Cross, P., 1998. The strain rate field in the eastern Mediterranean region, estimated by repeated GPS measurements. Tectonophysics, 294, 237-252.

Karaoğlu, Ö., 2014. Tectonic controls on the Yamanlar volcano and Yuntdağı volcanic region, western Turkey: Implications for an incremental deformation. Journal of Volcanology and Geothermal Research, 274, 16-33.

Karaoğlu, Ö., Helvacı, C., 2014. Isotopic evidence for a transition from subduction to slab-tear related volcanism in western Anatolia, Turkey. Lithos, 192-195, 226-239.

Kastelli, M., 1972. Denizli-Sarayköy-Çubukdağ-Karacasu alanı jeoloji incelemesi [in Turkish]. Mineral Research and Exploration Institute of Turkey (MTA), Report No. 2532, unpublished.

Kaymakcı, N., 2006. Kinematic development and paleostress analysis of the Denizli Basin (Western Turkey): Implications of spatial variation of relative paleostress magnitudes and orientations. Journal of Asian Earth Sciences, 27, 207-222.

Keller, E.A., 1986. Investigation of active tectonics: Use of surficial Earth processes. In: Wallace, R.E. (ed.). Active Tectonics. National Academy Press, Washington DC, 136-147.

Keller, E.A., Pinter, N., 2002. Active Tectonics: Earthquakes, Uplift, and Landscape. New Jersey, Prentice Hall, 362pp.

McKenzie, D., 1978. Active tectonics of the Alpine-Himalayan belt: the Aegean Sea and surrounding regions. Geophysical Journal of Royal Astronomic Society, 55, 217-254.

Kirby, E., Whipple, K.X., 2012. Expression of active tectonics in erosional landscapes. Journal of Structural Geology, 44, 54-75.

Konak, N., Göktaş, F., 2004. Geological maps of Turkey in scale of 1/100 000, Denizli M21 sheet [in Turkish]. Ankara, Mineral Research and Exploration Institute of Turkey (MTA) publications.

Kurt, H., Demirbağ, E., Kuşcu, İ., 1999. Investigation of the submarine active tectonism in the Gulf of Gökova, southwest Anatolia–southeast Aegean Sea, by multi-channel seismic reflection data. Tectonophysics, 305, 477-496.

Nebert, K., 1955. Bozdoğan ve Karacasu'daki genç Neojen körfezleri [in Turkish]. Mineral Research and Exploration Institute of Turkey (MTA), Report no 2511, unpublished.

Ocakoğlu, F., Dirik, K., Demirtaş, R., Özsayın, E., Açıkalın, S., 2007. Karacasu Ve Bozdoğan Çapraz Grabenlerinin (Batı Anadolu) Stratigrafik, Sedimantolojik Ve Tektonik Evrimi/ Stratigraphic, Sedimentologic and Tectonic Evolution of the Karacasu and Bozdoğan Cross-Grabens (western Anatolia) [in Turkish with English abstract]. Osmangazi University, Scientific Project No: 200415022, unpublished, 275pp.

Ocakoğlu, F., Açıkalın, S., Güneş, G., Özkes, S., Dirik, K., Özsayın, E., 2013. Was the 1899 Menderes Valley earthquake a double earthquake? Historical and paleosismological constraints. Journal of Asian Earth Sciences, 67-68, 187-198.

Ocakoğlu, F., Açıkalın, S., Özsayın, E., Dirik, K., 2014. Tectonosedimentary evolution of the Karacasu and Bozdoğan basins in the Central Menderes Massif, W Anatolia. Turkish Journal of Earth Sciences, 23, 361-385.

Ocakoğlu, F., Özsayın, E., Brook, G.A., 2015. Late Pleistocene-Holocene fluvial incision in the Karacasu graben (WAnatolia): an alternative approach to active tectonics of the Büyük Menderes graben. 6-10 April 2015, 68th Geological Congress of Turkey, Abstracts, 144-145.

Ouchi, S., 1985. Response of alluvial rivers to slow active tectonic movement. Geological Society of America Bulletin, 96, 504-515.

Ouimet, W.B., Whipple, K.X., Granger D.E., 2009. Beyond threshold hillslopes: Channel adjustment to base-level fall in tectonically active mountain ranges. Geology, 37(7), 579-582.

Özener, H., Doğru, A., Acar, M., 2013. Determination of the displacements along the Tuzla fault (Aegean region-Turkey): Preliminary results from GPS and precise leveling techniques. Journal of Geodynamics, 67, 13-20.

Özkaymak, Ç., 2014. Tectonic analysis of the Honaz Fault (western Anatolia) using geomorphic indices and the regional implications. Geodinamica Acta, 27(2-3), 109-128.

Özkaymak, Ç., Sözbilir, H., 2012. Tectonic geomorphology of the Spildağı high ranges, western Anatolia. Geomorphology, 173-174, 128-140.

Özsayın, E., 2016. Relative tectonic activity assessment of the Çameli Basin using geomorphic indices, Western Anatolia. Geodinamica Acta, 28(4), 241-253.

Papazachos, B.C., Comninakis, P.E., 1971. Geophysical and tectonic features of the Aegean arc. Journal of Geophysical Research, 76, 8517-8533.

Pérez-Peña, J.V., Azor, A., Azañón, J.M., Keller, E.A., 2010. Active tectonics in the Sierra Nevada (Betic Cordillera, SE Spain): Insights from geomorphic indexes and drainage pattern analysis. Geomorphology, 119, 74-87.

Pérez-Peña, J.V., Azañón, J.M., Azor, A., Booth-Rea, G., Galve, J.P., Roldán, F.J., Mancilla, F., Giaconia, F., Morales, J., Al-Awabdeh, M., 2015. Quaternary landscape evolution driven by slab-pull mechanisms in the Granada Basin (Central Betics). Tectonophysics, 663, 5-18.

Ramirez-Herrera, M.T., 1998. Geomorphic assessment of active tectonics in the Acambay graben, Mexican Volcanic Belt. Earth Surface Processes and Landforms, 23, 317-332.

Rockwell, T.K., Keller, E.A., Johnson, D.L., 1984. Tectonic geomorphology of alluvial fans and mountain fronts near Ventura, California. In: Morisawa, M. (ed.). Tectonic Geomorphology. Proceedings of the 15th Annual Geomorphology Symposium, Boston, Allen and Unwin Publishers, 183-207.

Sağlam-Selçuk, A., Kul, A.Ö., 2021. Long-term slip rate estimation for Erciş Fault in East Anatolian Compressive Tectonic Block from geologic and geomorphologic field evidence. Geological Journal, 56(10), 5290-5310.

Selby, M.J., 1980. A rock strength classification for geomorphic purposes: with tests from Antarctica and New Zealand. Zeitschrift für Geomorphologie, 24, 31-51.

Şengör, A.M.C., Yılmaz, Y., 1981. Tethyan evolution of Turkey: a plate tectonic approach. Tectonophysics, 75, 181-241.

Silva, P.G., Goy, J.L., Zazo, C., Bardaji, T., 2003. Fault-generated mountain fronts in southeast Spain: Geomorphologic

assessment of tectonic and seismic activity. Geomorphology, 50, 203-225.

Snyder, N.P., Whipple, K.X., Tucker, G.E., Merritts, D.J., 2003. Channel response to tectonic forcing: field analysis of stream morphology and hydrology in the Mendocino triple junction region, northern California. Geomorphology, 53, 97-127.

Soysal, H., Sipahioğlu, S., Kolçak, D., Altınok, Y., 1981. Historical earthquake catalogue of Turkey and surrounding area (2100 B.C.–1900 A.D.). Technical Report, The Scientific and Technological Research Council of Türkiye (TÜBİTAK), No. TBAG-341.

Strahler, A.N., 1964. Quantitative geomorphology of drainage basins and channel networks In: Chow, V.T. (ed.) Handbook of Applied Hydrology. New York, McGraw Hill Book Company, 439-476.

Sümer, Ö., İnci, U., Sözbilir, H., 2013. Tectonic evolution of the Söke Basin: Extension-dominated transtensional basin formation in western part of the Büyük Menderes Graben, western Anatolia, Turkey. Journal of Geodynamics, 65, 148-175.

Tepe, Ç., Sözbilir, H., 2017. Tectonic geomorphology of the Kemalpaşa Basin and surrounding horsts, southwestern part of the Gediz Graben, Western Anatolia. Geodinamica Acta, 29, 70-90.

Topal, S., 2019a. Evaluation of relative tectonic activity along the Priene-Sazlı Fault (Söke Basin, southwest Anatolia): Insights from geomorphic indices and drainage analysis. Journal of Mountain Science, 16(4), 909-923.

Topal, S., 2019b. Karacasu Fayı'nın (GB Türkiye) Göreceli Tektonik Aktivitesinin Jeomorfik İndislerle İncelenmesi [in Turkish with English abstract]. Gümüşhane Üniversitesi Fen Bilimleri Enstitüsü Dergisi, 9(1), 37-48.

Uzel, B., Sözbilir, H., 2008. A first record of a strike-slip basin in western Anatolia and its tectonic implication: The Cumaovası Basin. Turkish Journal of Earth Sciences, 17, 559-591.

Uzel, B., Sözbilir, H., Özkaymak, Ç., Kaymakçı, N., Langereis, C.G., 2013. Structural evidence for strike-slip deformation in the İzmir–Balıkesir transfer zone and consequences for late Cenozoic evolution of western Anatolia (Turkey). Journal of Geodynamics, 65, 94-116.

Wells, D.L., Coppersmith, K.J., 1994. New empirical relationships among magnitude, rupture length, rupture width, rupture area, and surface displacement. Bulletin of the Seismological Society of America, 84, 974-1002.

Wells, S.G., Bullard, T.F., Menges, C.M., Drake, P.G., Karas, P.A., Kelson, K.I., Wesling, J.R., 1988. Regional variations in tectonic geomorphology along a segmented convergent plate boundary pacific coast of Costa Rica. Geomorphology, 1, 239-265.

Westaway, R., Pringle, M., Yurtmen, S., Demir, T., Bridgland, D., Rowbotham, G., Maddy, D., 2003. Pliocene and Quaternary surface uplift of western Turkey revealed by long-term river terrace sequences. Current Science, 84(8), 1090-1101.

Whipple, K.X., DiBiase, R.A., Crosby, B.T., 2013. Bedrocks rivers. In: Shroder, J.F. (ed.). Treatise on Geomorphology. Poland, Elsevier, 550-573.

Whittaker, A.C, 2012. How do landscapes record tectonics and climate? Lithosphere, 4, 160-164.

Wobus, C., Whipple, K.X., Kirby, E., Synder, N., Johnson, J., Spyropolou, K., Crosby, B., Sheehan, D., 2006. Tectonics from topography: procedures, promise, and pitfalls. In: Willett, S.D., Hovius, N., Brandon, M.T., Fisher, D.M. (eds.). Tectonics, Climate and Landscape Evolution. Geology Society of America, 398 (Special Papers), 55-74.

Yılmaz, Y., Genç, Ş.C., Gürer, Ö.F., Bozcu, M., Yilmaz, K., Karacik, Z., Altunkaynak, Ş., Elmas, A., 2000. When did the western Anatolian grabens begin to develop? In: Bozkurt, E., Winchester, J.A., Piper, J.D.A. (eds.). Tectonics and Magmatism in Turkey and the Surrounding Area. London, The Geological Society, 173 (Special Publications), 353-384.

Yönlü, Ö., Altunel, E., Karabacak, V., 2010. Offset archaeological relics in the western part of the Büyük Menderes graben (western Turkey) and their tectonic implications. Geological Society of America, 471 (Special Papers), 269-279.